

Glycerol- and diglycerol-based polyesters: Evaluation of backbone alterations upon nano-formulation performance

Eleni Axioti^a, Emily G. Dixon^a, Morgan Reynolds-Green^a, Euan C.H. Alexander^b, Benedetta Brugnoli^c, Daniel J. Keddie^a, Benoit Couturaud^d, Jiraphong Suksiriworapong^e, Sadie M.E. Swainson^f, Iolanda Francolini^c, Steven M. Howdle^a, Philippa L. Jacob^{a,*}, Robert J. Cavanagh^{g,*}, Veeren M. Chauhan^{g,*}, Vincenzo Taresco^{a,*}

^a School of Chemistry, University Park, Nottingham NG7 2RD, United Kingdom

^b Department of Chemistry, Durham University, DH1 3LE, United Kingdom

^c Dept. of Chemistry, Sapienza University of Rome, Piazzale A. Moro 5, Rome 00185, Italy

^d Institut de Chimie et des Matériaux Paris-Est (ICMPE), CNRS, University Paris Est Créteil, UMR 7182, 2 Rue Henri Dunant, Thiais 94320, France

^e Department of Pharmacy, Faculty of Pharmacy, Mahidol University, Bangkok 10400, Thailand

^f Oral Product Development, Pharmaceutical Technology & Development, Operations, AstraZeneca, Macclesfield SK10 2NA, United Kingdom

^g School of Pharmacy, University of Nottingham, Boots Sciences Building, University Park, Nottingham NG7 2RD, United Kingdom

ARTICLE INFO

Keywords:
Glycerol
Diglycerol
Nanoparticles
Degradability
Polyesters
Amphiphilic balance

ABSTRACT

Despite the success of polyethylene glycol-based (PEGylated) polyesters in the drug delivery and biomedical fields, concerns have arisen regarding PEG's immunogenicity and limited biodegradability. In addition, inherent limitations, including limited chemical handles as well as highly hydrophobic nature, can restrict their effectiveness in physiological conditions of the polyester counterpart. To address these matters, an increasing amount of research has been focused towards identifying alternatives to PEG. One promising strategy involves the use of bio-derived polyols, such as glycerol. In particular, glycerol is a hydrophilic, non-toxic, untapped waste resource and as other polyols, can be incorporated into polyesters via enzymatic catalysis routes.

In the present study, a systematic screening is conducted focusing on the incorporation of 1,6-hexanediol (Hex) (hydrophobic diol) into both poly(glycerol adipate) (PGA) and poly(diglycerol adipate) (PDGA) at different (di)glycerol:hex ratios (30:70; 50:50 and 70:30 mol/mol) and its effect on purification upon NPs formation. By varying the amphiphilicity of the backbone, we demonstrated that minor adjustments influence the NPs formation, NPs stability, drug encapsulation, and degradation of these polymers, despite the high chemical similarity. Moreover, the best performing materials have shown good biocompatibility in both *in vitro* and *in vivo* (whole organism) tests. As preliminary result, the sample containing diglycerol and Hex in a 70:30 ratio, named as PDGA-Hex 30%, has shown to be the most promising candidate in this small library analysed. It demonstrated comparable stability to the glycerol-based samples in various media but exhibited superior encapsulation efficiency of a model hydrophobic dye. This in-depth investigation provides new insights into the design and modification of biodegradable (di)glycerol-based polyesters, potentially paving the way for more effective and sustainable PEG-free drug delivery nano-systems in the pharmaceutical and biomedical fields.

1. Introduction

A critical aspect for the application of (bio)polymers in pharmaceutical and biomedical fields is polymer degradation, as it can prevent the accumulation of hazardous materials within organisms and the

environment. [1,2] Aliphatic polyesters have been extensively studied and are capable of degradation through hydrolysis of ester bonds along the main backbone, or via enzymatic degradation, rendering them suitable materials in the field of drug delivery. [3–8] The rate and extent of degradation depends on polymer properties including

* Corresponding authors.

E-mail addresses: pippy.jacob@nottingham.ac.uk (P.L. Jacob), robert.cavanagh1@nottingham.ac.uk (R.J. Cavanagh), veeren.chauhan@nottingham.ac.uk (V.M. Chauhan), vincenzo.taresco@nottingham.ac.uk (V. Taresco).

<https://doi.org/10.1016/j.colsurfb.2024.113828>

Received 18 November 2023; Received in revised form 20 February 2024; Accepted 27 February 2024

Available online 28 February 2024

0927-7765/© 2024 The Authors. Published by Elsevier B.V. This is an open access article under the CC BY license (<http://creativecommons.org/licenses/by/4.0/>).

hydrophilicity/hydrophobicity, polymer chain length, nature of pendant side groups, and degree of crystallinity. [9,10] Poly(glycolic acid), poly(lactic acid) (PLA), and poly(ϵ -caprolactone) (PCL) are biocompatible materials that are widely used in pharmaceuticals and biomedical fields due to their physicochemical and mechanical properties. [9,11,12] While these materials do exhibit several advantageous properties, their applicability is limited due to their lack of chemical handles, restricted physicochemical properties, including high melting points and low solubility, and hydrophobic nature. Therefore, the degradation rate and consequently the responsiveness of the polymer in physiological conditions can be limited. In addition, due to the hydrophobic nature of such polymers, the use of these materials as nano-carriers is restricted unless copolymerised or functionalised along the backbone. [11,13,14] One widely studied method of modifying aliphatic polyesters involves their copolymerisation with polyethylene glycol (PEG) (PEGylation). PEGylation introduces a hydrophilic block into the polyester resulting in amphiphilic block copolymers capable of self-assembly into nanoparticles (NPs). [14–16] Despite the widespread use of PEG in drug delivery systems, concerns have been raised due to its limited biodegradation, tissue accumulation, and potential for immunogenicity. [17–19]

To circumvent these problems recent research has focused on identifying alternatives to PEG in the synthesis of amphiphilic degradable polyesters. [20] One synthetic strategy for producing polyesters is to replace the PEG segment with bio-derived polyols, such as sorbitol and glycerol *via* enzymatic catalysis routes. [21–24] This approach reduces reliance on petrochemical derived products, alleviates their negative environmental impacts, and contributes to a more sustainable biomaterials landscape. Glycerol is a major by-product of the biodiesel industry with a steadily growing production capacity of over 2 million tonnes per year predicted between 2023 and 2025, whilst enzymatic catalysis allows the production of controlled structures and retention of mild conditions. [25]

Among the glycerol-based polyesters reported in the literature, poly(glycerol adipate) (PGA) exhibits some of the key properties required to be considered a versatile polymeric carrier in drug delivery due to its intrinsic amphiphilicity facilitating self-assembly into polymeric NPs and drug encapsulation. [26–30] The unique chemoselectivity and regioselectivity provided by lipase (CaLB) enables the secondary hydroxyl group of glycerol to remain relatively unreacted and available as reactive pendant group. The control of self-assembly in a wide range of length scales may permit to tailor the nano- and micro-structure of materials thus optimising their performances in different fields, including drug delivery. [31,32] This eliminates the necessity for lengthy protection and deprotection steps and facilitates subsequent post-polymerisation functionalisation. [23,33–36] The main strategy adopted in the literature to promote amphiphilicity and introduce new functionality into PGA has been the modification of this free hydroxyl group. There are multiple examples in the literature where this moiety has been functionalised with a variety of molecules including fatty acids, drugs (e.g., indomethacin, mefenamic acid, methotrexate), cholesterol, tocopherol, folic acid, curable groups, amino acids, and PCL chains. [37–42] The nature and degree of substitution of the pendant group has been reported to influence PGA crystallinity, amphiphilicity, self-assembling ability, encapsulation efficiency, and the degradation profile of the polymers. [8] If the polymer functionalisation is not finely tuned, the post-polymerisation functionalisation can hinder the unique, beneficial properties that PGA is known to exhibit.

To minimise these synthetic limitations and expand the chemical space explored in the enzymatically synthesised PGA-based polyesters, our group has previously introduced a straightforward one-pot synthetic modification. [29,36,43] A small library of functionalised diols was used in combination with glycerol - introducing a variety of functional groups as well as hydrophobic linkers into polymer backbone while retaining the glyceryl secondary hydroxyl group. The incorporation of hydrophobic 1,6-*n*-hexanediol (Hex) enhanced the ability of the polymer to

self-assemble and encapsulate a model hydrophobic small molecule. In a similar fashion, by recently focusing on branched glyceride-like polyesters, Perin et al., have shown that by modifying the nature of the diacid counterpart, it is possible to alter amphiphilicity, physical properties, and ability of such polymers to self-assemble into NPs. [33] On this basis, we have expanded these works by demonstrating that the incorporation of the more hydrophilic diglycerol, instead of glycerol, further enhanced the ability of the polyesters to encapsulate hydrophobic small molecules. [44,45]

However, in all previous examples, the focus of the variation of the polymer backbone was on a single ratio of (di)glycerol:diol, 50:50 mol/mol. While this provided useful insight into the benefits of rebalancing the amphiphilicity of these polyesters, a more in-depth screening of amphiphilicity rebalancing has not been conducted.

For this reason, in the present work we have performed a methodical screening of the effect of the incorporation of Hex into both PGA and poly(diglycerol adipate) (PDGA). Ratios of (di)gly:hex at 30:70, 50:50, and 70:30 mol/mol were investigated. Additionally, both the impact of diol ratios and subsequent polymer purification, through various precipitation steps, have been examined on the resulting physicochemical properties of both the polymers and nanoparticles (NPs). Through these modifications, we prove that the self-assembling properties of PGA and PDGA-based polymers are significantly influenced by the minor alteration of amphiphilicity in the polymer chain. This systematic screening enhances our understanding of amphiphilic balance effects polyester properties and related behaviour of their self-assembling NPs.

2. Materials and methods

2.1. Materials

Divinyl adipate (DVA) was purchased from Tokyo Chemical Industries, UK. Glycerol, diglycerol and 1,6-*n*-hexanediol (Hex) were purchased from Sigma-Aldrich, UK. Phosphate buffer saline (PBS), bovine serum albumin (BSA), coumarin 6, Novozym 435 lipase, derived from *Candida antarctica* immobilised on an acrylic macroporous resin, were also purchased from Sigma Aldrich. Solvents were purchased from Fisher Scientific UK (tetrahydrofuran, 2-methyltetrahydrofuran, diethyl ether, hexane, and ethanol) and Sigma Aldrich (acetone, acetone d₆), and were used without further purification. All chemicals and solvents were used as received without further purification.

2.2. Characterisation

2.2.1. Nuclear magnetic resonance spectroscopy (NMR)

Successful polymer synthesis was confirmed using ¹H NMR spectroscopy. NMR spectra were recorded using a Bruker DPX 400 MHz spectrometer using acetone-*d*₆ solvent. Chemical shifts are given in ppm. Approximately 5 mg of polymer was dissolved in 0.6–0.7 mL of the solvent. MestReNova 14.3.2 copyright 2023 (Mestrelab Research S.L.) was used for analysis.

2.2.2. Gel permeation chromatography (GPC)

Polymer Number Average Molar Mass (M_n) and dispersity (D) were determined using GPC in THF (HPLC grade) eluent at 40 °C. Chromatographs were recorded using two Agilent PL-gel mixed D columns in series with a flow rate of 1 mL min⁻¹ and an injection loop of 50 μ L. Samples were detected using a differential refractometer (DRI). Samples were prepared by dissolving sample (6 mg) in THF (2 mL) and filtering through 0.22 μ m Teflon filter. Low dispersity (D) poly (methyl methacrylate) standards were used for the system calibration with average molar masses ranging from 540 to 1.02×10^6 g mol⁻¹.

2.2.3. Differential scanning calorimetry (DSC)

Thermal properties of the polymers were determined using DSC. Analysis was performed on a TA-Q2000 (TA instruments), calibrated

with sapphire and indium standards under N₂ flow at 50 mL min⁻¹. Polymer (~5 mg) was weighed into a T-zero aluminium pan (TA instruments) with a reference pan (T-zero aluminium) remaining empty. Pan lids were pin-holed, due to the stickiness of the polymer, and samples were heated at a rate of 10 °C min from -90 to 200 °C. Two heating cycles were recorded in order to remove any thermal history of the polymers. The second heating cycle was used to determine the glass transition temperature (T_g) and melting temperature (T_m) of polymers.

2.2.4. Water contact angle measurement (θ_w)

Water contact angle samples were prepared by solvent casting of polymer from a solution of acetone onto microscopic glass slides. Samples were prepared at a concentration of 3 mg/mL using the film technique, by pipetting 3–4 drops of polymer solution onto the whole surface of the glass slides and letting the solvent evaporate overnight. Water contact angles were measured using a KSV Cam 200 (KSV Instruments Ltd, Helsinki, Finland) equipped with CAM200 software. Samples were measured at a constant temperature (25 °C) with at least three replicates of each measurement recorded at two different time points, $t=0$ (the exact moment when water touches the polymer surface) and $t=5$ sec (as soon as the drop settles on the surface).

2.3. Polymer synthesis

For PGA synthesis, the published protocol was followed. [44] In a 20 mL vial, glycerol (12.50 mmol) and DVA (12.50 mmol) were weighed and dissolved in 2-MeTHF (10 mL). Novozym 435 (0.11 g, 4.4%w/w compared to DVA) was added to all the mixtures, which were then stirred at 200 rpm at 50 °C for 5 h in a sealed vial, with the rubber septum being pierced with two needles to allow the release of acetaldehyde, a by-product of the reaction. After 5 h, the reaction was stopped by removal of the enzyme by filtration. The solvent was removed under reduced pressure. The polymer was kept under reduced pressure at 25 °C for a week to remove residual solvent leaving a viscous, pale-yellow polymer. The polymer conversion was quantitative, as confirmed by ¹H NMR spectroscopy.

For the hexanediol-variants, according to the published protocol, [44] synthesis occurred by weighing 1,6-*n*-hexanediol (6.25 mmol), glycerol (6.25 mmol) and DVA (12.50 mmol) into a 20 mL glass vial and dissolving in 2-MeTHF (10 mL). This ratio glycerol:hexanediol 50:50, will be further referred to as PGA-Hex 50% (% is always referred to the amount of Hex in the polymers). 30% (PGA-Hex 30%) and 70% (PGA-Hex 70%) hexanediol variants were prepared with 3.75 mmol and 8.75 mmol hexanediol respectively, and the moles of glycerol adjusted according to $M_{\text{glycerol}} + M_{\text{hexanediol}} = 12.50$ mmol.

A revised procedure was followed for PDGA based polymers; diglycerol is poorly soluble in 2-MeTHF, therefore THF was used instead.

PGA: 1.65 (4 H, s), 2.37 (4 H, s), 4.02–4.24 (5 H, m, 1,3 disubstituted glycerides), 5.08 (fraction of 1 H, m, 1,2 disub) and 5.28, 5.35 (fraction of 1 H, m, 1,2,3 trisub)

PGA-Hex 50%: 1.40 (2 H, m) 1.64 (4 H, s), 2.35 (6 H, s), 4.02–4.23 (5 H, m, 1,3 disubstituted glycerides), 5.08 (fraction of 1 H, m, 1,2 disub) and 5.28, 5.35 (fraction of 1 H, m, 1,2,3 trisub)

PDGA: 1.66 (4 H, s), 2.36 (4 H, s), 3.43–4.39 (10 H, m 1,3 disubstituted diglycerides), 5.01 (fraction of 1 H, m, 1,2 disub) and 5.20 (fraction of 1 H, m, 1,2,3 trisub)

PDGA-Hex 50%: 1.40 (2 H, m) 1.64 (4 H, s), 2.34 (6 H, s), 3.43–4.39 (10 H, m 1,3 disubstituted diglycerides), 5.00 (fraction of 1 H, m, 1,2 disub) and 5.19 (fraction of 1 H, m, 1,2,3 trisub)

2.4. Polymer purification

Purification by fractionated precipitation of a solution of polymer into a non-solvent for the polymer should provide the removal of low molar mass entities and shorter oligomers, leaving the longer and more uniform chains. After complete dissolution of the polymer (250 mg) in

acetone (1 mL), the precipitation was performed in a series of non-solvents, hexane, diethyl ether, a mix of these two at 50:50 ratio, and methanol (15 mL). The precipitated materials were collected by centrifugation and after removal of the supernatant, the pellets containing the purified polymers were dried in a vacuum oven to remove the residual solvent and subsequently analysed (Table S1).

2.5. NPs formulation and characterisation

2.5.1. NPs formation

NPs were prepared by nanoprecipitation. Briefly, polymer (10 mg) was dissolved in acetone (2 mL) and then added dropwise into deionised water (4 mL) under constant stirring at 500 rpm. The uncapped solutions were left stirring overnight to allow for complete evaporation of acetone. The final NPs concentration was 2.5 mg/mL. Samples were analysed for size and zeta potential before and after filtration (0.22 μm) using cellulose filters.

2.5.2. Dynamic light scattering (DLS) and zeta potential measurements

Dynamic light scattering was used to determine NPs size using a Zetasizer Nano spectrometer (Malvern Instruments Ltd.) equipped with a 633 nm laser at a fixed angle of 173° and a Wyatt DyanPro DLS Plate Reader. Samples were equilibrated for 30 s at 25 °C prior to measurement. Zetasizer Nano spectrometer was also used to measure zeta-potential of the NPs. All samples were measured in triplicate. NPs were prepared at a concentration of 2.5 mg/mL and measurements were done in both samples that were unfiltered and filtered through 0.22 μm filter.

2.5.3. Coumarin encapsulation and fluorescence microscopy

Coumarin (Cou6) solutions (1 mg/mL) were prepared in acetone. Polymer (10 mg) was weighed into a vial and dissolved in coumarin solution (1 mL). In this way, formulations with a polymer:cou6 ratio, by weight, of 10:1 were prepared. Polymer solutions were subsequently added dropwise into deionized water (4 mL) whilst stirring at 500 rpm. Vials were left under stirring overnight to enable acetone evaporation. Nanoparticle-dye dispersions were filtered through a 0.22 μm filter. Coumarin blank was filtered and measured in water without the addition of polymer. Particle sizes and Z-potential were determined using DLS. In addition, the encapsulation was qualitatively determined using fluorescence spectrophotometry, by measuring the fluorescence intensity of the NPs-dye dispersions at excitation wavelength $\lambda = 460$ nm and emission wavelength $\lambda = 500$ nm.

$$\Delta F\% = \frac{\Delta F}{F} = \frac{(F_{\text{NPs}} - F_{\text{Cou6}})}{F_{\text{Cou6}}} \times 100$$

F_{NPs} = fluorescence signal of NPs formulation with encapsulated Cou6, normalised by the polymer F.

F_{Cou6} = fluorescence signal of the free dye in water

2.5.4. NPs stability in BSA and PBS

Stock solutions of polymers were prepared at 2.5 mg/mL. Stock solution of bovine serum albumin (BSA) was prepared at 2 mg/mL in DI water, following the published protocol. Stock solution of phosphate buffered saline (PBS) was prepared at 3 mg/mL in DI water. The polymer solutions (100 μL) were mixed with BSA (100 μL) and PBS (100 μL) in a well plate. Samples were measured in a DLS plate reader at $t = 0, 3,$ and 24 h to assess the stability of NPs.

2.5.5. Enzymatic degradation/hydrolytic enzymatic assay

Lipase from porcine pancreas, Type II (≥ 125 units/mg protein (using olive oil (30 min incubation)), 30–90 units/mg protein (using triacetin)) was used in this experiment. A solution of enzyme at 10 mg/mL in PBS was prepared. 50 μL of this solution were added to 250 μL of NPs (at concentration of 2.5 mg/mL in water, as mentioned previously). The effect of the enzyme was observed within 24 h at 25 °C.

2.5.6. Transmission electron microscopy (TEM) measurements

NPs suspensions (13 μ L, 2 mg/mL) were added to a copper grid (Carbon film 200 mesh copper (Agar Scientific)) and left for 2 min after which time the excess sample was removed. The TEM grids were left to dry for 3 h before measuring. Analysis was performed using a FEI Biotwin-12 TEM fitted with a digital camera.

2.6. In vitro cell culture

The human intestinal epithelial adenocarcinoma cell line Caco-2 was obtained from the American Type Culture Collective (ATCC) and used between passages 40–50. Cells were cultured in Dulbecco's Modified Eagle Medium (DMEM) supplemented with 10% Fetal Bovine Serum (FBS) at 37 °C in a humidified incubator with 5% CO₂. Cells were routinely grown in 75 cm² culture flasks to 70% confluence.

2.7. In vitro PrestoBlue metabolic activity assay

Cellular metabolic activity was measured using the PrestoBlue viability assay (Thermo Fisher Scientific) as an indication of cytotoxicity. Caco-2 cells were seeded at 1×10^4 cells per well in 96 well plates and cultured for 24 h. After 24 h, they were exposed to treatments in 100 μ L phenol red free DMEM for 24 h. Triton X-100 was applied at 1% (v/v) as positive cell death control and medium alone was used as negative control. Following exposure period treatments were removed and cells incubated with 100 μ L 10% (v/v) PrestoBlue reagent per well, diluted in phenol red free medium for 60 minutes. The resulting fluorescence was measured on a Tecan Spark 10 M plate reader at an excitation wavelength $\lambda = 560$ nm and emission wavelength $\lambda = 600$ nm. Relative metabolic activity is calculated from PrestoBlue data by setting values from the negative control as 100% and positive control values as 0% metabolic activity (Equation 1)

$$\text{Relative metabolic activity} = \left(\frac{(x - \text{Positive control})}{(\text{Negative control} - \text{Positive control})} \right) \times 100$$

Equation 1. Calculation of relative metabolic activity. x = treated sample fluorescence value. All values are from fluorescence at 560/600 nm ($\lambda_{ex}/\lambda_{em}$).

2.8. In vitro LDH release test

To study plasma membrane damage *in vitro*, the extracellular release of lactose dehydrogenase (LDH) enzyme was assessed using the LDH release assay (Sigma Aldrich, TOX7 kit) As above, Caco-2 cells were seeded at 1×10^4 cells per well in 96 well plates and cultured for 24 h. Cells were exposed to treatments in 100 μ L phenol red free DMEM and received either polymeric formulations, 1% Triton X-100 to induce cell lysis or DMEM only to serve as the vehicle control. Following 24 hours exposure, 50 μ L of supernatant per well was sampled and transferred to a new 96 well plate for detection of LDH released extracellularly. LDH detection solution was prepared according to the manufacturer's instructions and 100 μ L detection reagent added per well to the 50 μ L of supernatant sample. The solution was incubated at room temperature protected from light for 25 minutes and the absorbance of the resulting solution measured at 490 nm on a Tecan Spark 10 M plate reader. Relative LDH release was calculated by setting the absorbance signal of 1% Triton X-100, assumed to generate full cell lysis, as 100% LDH release and the background signal generated by LDH detection solution alone as 0%.

2.9. C. elegans in vivo cytotoxicity

In vivo toxicity was investigated by challenging *Caenorhabditis elegans* nematodes to polymers PGA-Hex (30% & 50%, 0.5 mg/mL), and

PDGA-Hex (30% & 50%, 0.5 mg/mL). Adult *C. elegans* were filtered (Merk 20 μ m Nylon filter) and washed with M9 buffer solution (50 mL). Nematodes (> 40 animals) were made up with 0.5 mg/mL of polymer, suspended in M9 buffer solution, with 0.1 OD₆₀₀ of *Escherichia coli* for sustenance. Controls were used for experimental guidance in the form *E. coli* alone (positive control) and absolute ethanol (20% v/v, negative control). Nematodes were imaged at Time = 24 h. All experimental conditions were conducted in triplicate, and error shown on data is standard deviation. Viability of nematodes was determined according to motile percentage calculations. [46] An absolute indicator of nematode viability was also determined through the observation of progeny production after 24 h.

2.10. Statistical analysis

NPs stability from different solvents and over time (Figs. 2A and 2B) and cytotoxicity results for *in vitro* cell culture were tested for significant differences from control group (DMEM) using two-way ANOVA and Dunnett's multiple comparisons post-hoc test. For *in vivo* *C. elegans* cytotoxicity significance was tested using Student's T test. Statistical significance was determined at $P < 0.05$.

3. Results and discussion

3.1. Polymer synthesis

PGA and PGA-Hex variants (Scheme S1) were successfully synthesised using the sustainably resourced solvent 2-MeTHF. [47–49] This was confirmed by both GPC and ¹H NMR (Figure S11) and comparing to the existing literature. Full ¹H NMR peak assignment has been described by Taresco *et al.* (2016) [36] and Jacob *et al.* (2021). [43] Divinyl peaks initially present in the DVA monomer at 4.59, 4.87 and 7.29 ppm disappeared due to esterification and removal of side product acetaldehyde. [29,50] As previously reported, [36] protons relating to glyceride peaks appeared between 3.5 and 4.4 ppm, indicative of the esterification of the glycerol hydroxyl groups. Glycerol and adipic peaks also shifted and broadened in shape relative to the monomers alone. These factors combined confirm successful polymerisation(s). Despite the primary alcohol selectivity of the lipase, a small percentage of secondary hydroxyl groups of glycerol had participated in polycondensation (likely due to the unconventional temperature and use of organic solvent), [33] the representative peaks labelled as c' and c'' , respectively (INSET left, Figure S11).

The c' peak at 5.08 ppm relates to 1,2-disubstitution (not reported in the scheme but reported previously in literature [36]), as this still provides a linear polymeric backbone, this peak is not included in the branching percentage. The c'' peak at 5.28 ppm corresponds to the 1,2,3-trisubstituted glycerol units (not reported in the scheme but reported previously in literature [36]) and was calculated as a branching mol/mol%, as reported previously. [36,44] A small, additional branching peak at 5.35 ppm was visible for all four polymers and may correspond to methine protons on secondary glycerides trisubstituted with a different environment and was included in the calculation for c'' . As expected, percentage of 1,2,3-trisubstituted glyceride (branching) of the polymer backbone decreased as the mole percentage of Hex was increased, due to less glycerol present. Additionally, the glyceridic peak at 4.12 ppm (c,d) decreases with increasing hexanediol. In the ¹H NMR spectra of the PGAHex-based polymers, the peak at 1.63 ppm, labelled b and y , is comprised of 4 adipic protons and 4 methylene protons of hexanediol (INSET right, Figure S11). The integrals of these protons are in agreement with the molar ratios of diols used in the polymer syntheses. For PGA-Hex 30%, the expected integral at 1.63 ppm is 5.2. This value is the result of 4 (adipic) protons and 4×0.3 equivalents $-CH_2$ of hexanediol proton, y (Figure S11) when the adipic peak at 2.36 ppm is set to be equal to 4 protons. The measured integral of 5.12 is in agreement with the expected value.

PDGAHex-based polymers produced (in THF due to the low solubility of diglycerol in 2-MeTHF) were analysed by ^1H NMR (Figure SI2) as previously reported in the literature (full analysis has been performed by [44]) As expected, with the addition of more Hex, a decrease in the diglyceride peak intensity at 3.5–4.1 ppm occurs as the mole percentage of diglycerol decreases, as was also shown for glycerol. The extent of trisubstitution on the pendant OH group has been found to be <10% mol/mol and decreases with increasing hexanediol content, as was also seen for PGA based polymers (Figure SI2). This low level of trisubstitution can be achieved thanks to the use of Novozym 435 as chemo- and regio-selective catalyst, reacting preferentially with primary hydroxyl groups. In fact, it is widely reported that when glycerol is used as a monomer for the synthesis of polyesters via thermal polycondensation (temperature $\geq 120^\circ\text{C}$) cross-linked networks can be produced. [51,52] However, when an enzymatic catalysis route is selected, cross-linking is avoided even at high monomer conversion but, as demonstrated herein a low degree of branching can be expected. [53,54] Generally, the level of trisubstitution is lower in diglycerol based polymers compared to glycerol-based analogues due to the high steric hindrance provided by the two vicinal pendant hydroxy groups when an immobilised lipase is used as catalyst, as also shown previously. [44] As for the PGA Hex-based polymers, the diglycerol:Hex ratio has been evaluated and confirmed via ^1H NMR spectroscopy (Figure SI2).

3.2. Molar mass analysis

GPC traces showed a broad ($1.5 \leq D \leq 2.10$) polymeric peak for each derivative, ranging from M_n 3600 up to 5400 g mol^{-1} and traces of oligomers, as previously observed in literature. [44] In addition, PDGA showed a lower molar mass, due to its shorter chain length. This is likely caused by the increased viscosity of diglycerol and therefore slow reaction kinetics in the same reaction time as well as lower branching. A finding that was in line with the literature. [44] The molar masses of the Hex-based polymers were found to be higher than unmodified PGA and PDGA (Table 1). [44] This may be due to a higher solubility of hexanediol in THF in comparison to the hydrophilic polyols, facilitating hexanediol to react and therefore, higher molar masses. Moreover, for the glycerol/diglycerol variants, increasing the amount of hexanediol from 30% to 50% results in a rise in the molar mass, while the following increase of 50–70% leads to a decrease in the molar mass. This is likely explained by the fact that when increasing the amount of Hex, above the 50% threshold, although the complete polymerisation is promoted, more oligomers can be produced due to the excess of hexanediol. Furthermore, the addition of more Hex has an effect on final polymer

Table 1

Number average molar mass (M_n), D , T_g , T_m and ΔH_m .

Polymer	M_n (g mol^{-1}) ^a	D (M_w/M_n) ^a	T_g ($^\circ\text{C}$) ^b	T_m ($^\circ\text{C}$) ^b	ΔH_m (J g^{-1}) ^b
PGA	4.8×10^3	2.10	-28.2	N/A	N/A
PGA-Hex 30%	5.9×10^3	1.90	-39.7	N/A	N/A
PGA-Hex 50%	6.1×10^3	1.70	-49.8	10.8, 24.5	5.0, 13.4
PGA-Hex 70%	4.4×10^3	1.70	-50.1	32.3, 37.0	48.4
PDGA	3.6×10^3	1.50	-17.6	N/A	N/A
PDGA-Hex 30%	5.0×10^3	1.80	-28.4	N/A	N/A
PDGA-Hex 50%	6.9×10^3	1.80	-38.9	24.5	2.2
PDGA-Hex 70%	6.0×10^3	1.70	-40.1	29.5, 37.6	11.0, 16.3

^a Molar mass was determined by GPC using THF eluent at 40°C . GPC was calibrated using low dispersity PMMA standards with molar mass ranging from 540 to 1.02×10^6 g mol^{-1} .

^b Thermal properties determined by DSC.

solubility and linearity. Therefore, we postulate the detected molar mass is due to a different elution volume of the polymer bearing 70% of Hex.

3.3. Thermal properties

DSC analysis was used to further confirm the success of the polymerisation of all variants (Table 1) when compared to the known literature. [43,44,55,56] Regarding the thermal analysis, polymers without Hex were found to be completely amorphous, with T_g values ranging from -40 to -20°C (Table 1), while the hexanediol-modified glycerol/diglycerol variants showed both a T_g in the region between -50°C and -30°C (Table 1) and weak melting transitions between 10 and 37°C (Table 1). The melting peaks cannot be appreciated when the amount of Hex is below 30%, while two melting peaks can be observed in most of the other Hex variants, suggesting the presence of either small traces of unreacted Hex or two possible polymorphs due to the heterogeneity of the polymer backbone. In general, the use of hexanediol decreased the polymer T_g further with respect to the pure PGA. All polymers maintain good flexibility at room or body temperature as all the T_m s are below or around 37°C .

3.4. Water contact angle (Θ_w)

The water contact angle is adopted as a qualitative way to evaluate whether the surface has a hydrophobic or hydrophilic characteristic. [57] As expected, as the hexanediol ratio increased, the hydrophobicity of the final polymer increased almost in linear fashion (Figure SI3). However, all the Θ_w measured were below the conventional hydrophobic threshold of 90° hinting at a generally hydrophilic surface. We observed that as soon as the water droplets reached the polymer surfaces (Figure SI3, $t=0$ s), the polymers with the lower hexanediol amounts showed smaller contact angles. In addition, when the droplets settled on the polymer surface (Figure SI3, $t=5$ s) a rearrangement of the surface occurred, presumably, causing the -OH to segregate (reassembling/-rearranging) towards the droplet, leading the droplet to flatten/spread out and "wet" the surface more. This is likely due to increased hydroxyl moieties that could rearrange and interact with the droplet. This time-related wetting behaviours and related hydroxyl groups/polar moieties rearrangement towards the water droplets may be used as further evidence of the amphiphilic nature of the polymeric materials. Finally, the largest change with the subsequent largest drop in contact angle was observed for the PDGA variants corroborating the hypothesis that more hydroxyl groups may be able to rearrange towards the water droplet.

3.5. Purification results – PGA-Hex 50% polymers

In order to understand the effect of polymer purification (via direct polymer precipitation) upon chemical properties and self-assembling ability of the polymers, four different (non)solvent systems with different polarity properties; hexane, diethyl ether, a mix of these two at 50:50 ratio, and methanol were used. Showing PGA-Hex 50% as an example: ^1H NMR analysis of PGA-Hex 50% was repeated after purification in the solvent mixtures (Fig. 1). Overall, the polymer structure remained consistent throughout, with no structural change in the polymer visible in the ^1H NMR analysis and with unchanged glycerol:hex ratios. However, the level of 1,2,3-trisubstitution slightly changed only for the case of purification in Hexane (Fig. 1, inset), likely due to selective removal of more linear fraction.

GPC proved that although the M_n and D of the purified polymers remained largely the same (Table SI1) for the more non-polar mixtures (hexane, diethyl ether, and the 50:50 ratio mix), the purification step using the more polar methanol allowed the full removal of low molar mass shoulders, likely due to oligomers (Figure SI4 and Table SI1). This resulted in the fractioning and selection of a higher molar mass/DP and well-defined peak (Figure SI4) with lower solubility in the polar solvent,

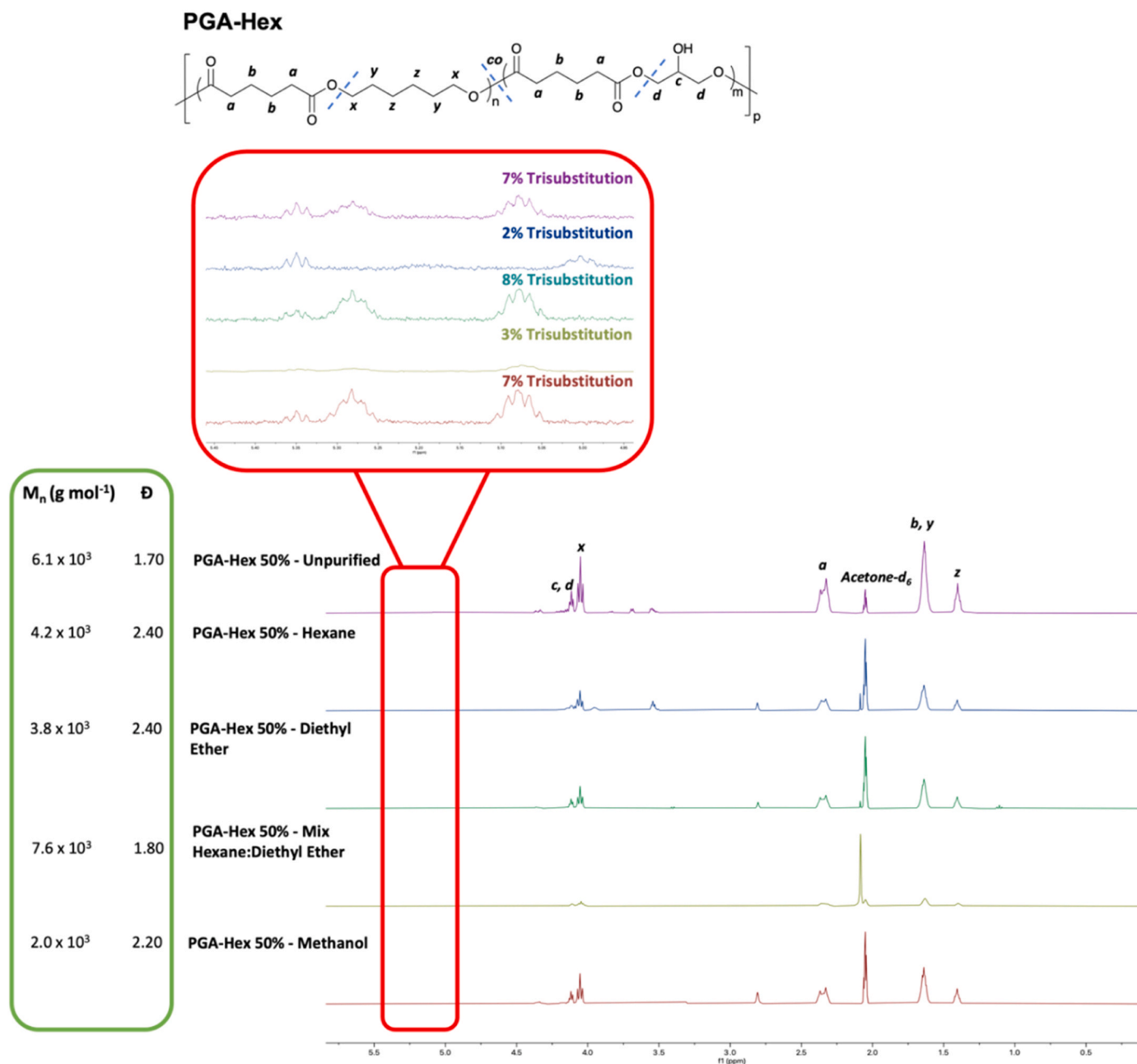


Fig. 1. ¹H NMR spectra with corresponding GPC data for PGA-Hex 50% and subsequent purifications. Branching structure on the polyester backbone is not shown for clarity. Inset shows degree of 1,2 disubstitution (c') and 1,2,3 trisubstitution (c'). Blue dashes represent that the diols in the polyester backbones may not be repeating sequentially. Levels of trisubstitution is reported inset.

methanol. However, the yield of the precipitation step from methanol was low (Table SI1), due to a large proportion of the polymer chains being soluble in the non-solvent and only worked for the glycerol-based polymers. In addition, to confirm this observation, other polar solvents were used for the diglycerol-based polymers, ethanol and ethyl acetate. Regardless of the change in polarity, the yields remained at low levels (Table SI1).

Moreover, when testing the self-assembly behaviour of the purified PGA-Hex 50 from the different non-solvents, it was observed that the size of NPs before and after purification still ranged within the same size range (130–145 nm) (Figure SI5). Only when methanol was used, the NPs produced were slightly smaller in the range of roughly 90 nm. Despite this, the size distribution was broader (PDI = 0.107) than the non-purified, which was as narrow as 0.037. Considering the experimental evidence, purification with polar solvents fractionate longer

chain entities and reducing branched species, however it does not enhance the self-assembly properties of the polymers. Therefore, purification is an extra procedural step that leads to use and waste of toxic, hazardous solvents and consequently can be avoided, in the interest of a more sustainable process.

3.6. NPs formation and solvent analysis

In the nano-formulation screening, PGA and PDGA have been excluded according to previous literature assessment of their poorer performances when compared to their Hex polyester variants.⁴⁴

All the unpurified polymers synthesised in this work have been tested for their ability to form NPs according to the protocol previously applied in the literature for similar polymers. [58] To optimise the NPs formation, two solvents were used for the nanoprecipitation technique:

acetone and THF. [59] The nanoprecipitation technique is a complex process, which can be affected by many factors, including water-solvent miscibility and polymer nature. [60] THF gave slightly larger PDGA-Hex NPs sizes than acetone due to different water-solvent miscibility. THF has lower dielectric constant and solubility parameter than acetone, suggesting that the difference in water-THF miscibility was greater than that in the case of acetone. Lower water-solvent miscibility hindered water-solvent blending rate and thus, leading to larger NPs size. [61]

Although at $t=0$ (after overnight solvent evaporation) NPs sizes are similar for both solvents, after $t=1$ week all the NPs prepared using THF showed both instability (with some noticeable precipitation), substantial and very significant ($P<0.001$) enlargement of sizes via DLS (Fig. 2A). On the other hand, the NPs prepared using acetone showed no evident precipitates after 1 week. Size consistency was visible over the stability period throughout the PDGA series, regardless of the amount of Hex. While, in the PGA series, a statistical difference in average size after 1 week it has been seen, however, the size did not vary more than 10 nm. It is notable that PDGA-Hex polymer NPs were smaller than PGA-Hex analogues from $t=0$. For this reason, it was decided to continue the NPs production and screening using acetone alone. To further probe the behaviours of the produced NPs, stability up to a month was also investigated (Fig. 2B). Regardless Hex amount, all polymeric NPs showed good stability, with limited size enlargement over the observed timeframe and with differences in average sizes between time zero and $t=1$ month always below 40 nm. In addition, all NPs sizes were below 200 nm (ranging from ~ 90 –150 nm) (Fig. 2B).

However, both polymers prepared with the higher amount of Hex, PGA-Hex 70% and PDGA-Hex 70%, respectively, produced aggregates when formulated via nanoprecipitation at 2.5 mg/mL and from both acetone and THF (Figure S16). With the aim of performing an explorative screening of the effect of hydrophobicity effect of polymer backbone upon NPs formation, these two polymers were excluded from further analysis.

3.7. NPs stability in biological conditions

To investigate the NPs stability and stealth-like properties in biological-like conditions, bovine serum albumin (BSA) was used as a model protein similar to the one in the human blood stream. [62,63] Phosphate Buffered Saline (PBS) was also investigated due to having ionic strength similar to cell culture media and human fluids. [64,65] NPs of the two ratios (30% and 50%) for both PGA-Hex and PDGA-Hex stability through DLS measurements were investigated (Fig. 2C). Out of all the NPs, PGA-Hex 50% appears to be the most stable of the polymers synthesised. This is due to the higher hydrophobicity of this polymer compared to the other three samples, allowing a better NPs hydrophobic core packing with consequent formation of a stable hydration shell and enhanced stability of the nano-dispersion in aqueous media. Particle sizes of PGA-Hex 50% remained unchanged for all time points in presence of PBS and only a slight change in the intensity when using BSA in testing environment (Fig. 2C). Particle sizes of PDGA-Hex 30% and 50% tended to remain unchanged after 24 h in BSA. PDGA-Hex 50% showed instability in PBS and size broadening after 3 h. However, both polymers afforded markedly size changes at the last time point of $t=24$ h (Fig. 2C). The differences in stability between PGA polymers and the PDGA set may be traceable again to the higher hydrophobicity and higher Θ_w values of the polymers bearing glycerol. The improved hydrophobic character may provide a more stable core which could lead to more stable NPs. On the other hand, the presence of diglycerol may lead to more water-soluble polymers with more unbound NPs cores, which are destabilised by the presence of higher ionic strength in PBS. [66] However, these tests have been conducted to gather initial qualitative information on size variation in different media in order to identify a fast screening system. For this reason, statistical analysis on this data was not performed.

3.8. NPs qualitative degradation assay

In order to acquire knowledge on the behaviour of the prepared NPs in the presence of a common lipase (details in Materials and Methods), DLS was used as a rapid screening technique, monitoring the change in nanoparticle size after enzyme addition. This experiment was conducted to provide an indication of whether or not a lipase would degrade the produced polymers, rather than a quantitative measure of the degree of degradation as already suggested by the literature. [8] It has been previously shown that the increase in particle size is due to swelling, followed by the aggregation of the NPs, which can be taken as a sign of degradation. [67] In fact, before (Alone) and just after adding the enzyme ($t=0$, at 25 °C) only a single peak is observed, reflecting the well-defined and monodisperse NPs (Fig. 3 Alone and $t=0$ at 25 °C). As the degradation progresses, the polyester chains are hydrolysed with consequent formation of shorter and more hydrophilic chains within the NPs first swelling and then aggregating (after 30 min, 5 h and 24 h respectively at 25 °C).

All polymers tested showed fast interaction with the enzyme with swelling evident within the first 30 mins and remarkable size enlargement, hinting at aggregation from 5 h onwards (sizes $>3 \mu\text{m}$) (Fig. 3). This increment in size was significantly different to the behaviour observed in PBS after the same observation timeline (Figs. 2 and 3). Additionally, attenuator values were automatically selected by the instrument, moving from approximately 6 ($t=0$) to 9 (after 24 h), for all the samples. This means that the concentration of the material able to scatter the light in the sample had decreased, again indicating degradation and/or aggregation. However, due to the nature of the measurement, this can be considered only as qualitative analysis of the interactions between the NPs and lipase.

3.9. NPs toxicity testing

3.9.1. *In vitro*: intestinal epithelial

To assess the cytocompatibility of PGA-Hex and PDGA-Hex NPs systems generated via nanoprecipitation with acetone, human intestinal Caco-2 cells were exposed for 24 hours to 0.125, 0.25 or 0.5 mg/mL of the polymeric formulations (Fig. 4). The resulting metabolic activity was then probed as an indication of cell viability (Fig. 4A) and extracellular release of LDH enzyme measured to evaluate potential plasma membrane damage (Fig. 4B). The data demonstrate that the applied systems are non-toxic, as indicated by no decreases in cellular metabolic activity and no substantial differences in LDH release when compared to the vehicle control (DMEM); statistical analysis using two-way ANOVA test determined no significant difference between test systems and DMEM control in both assays ($P > 0.05$). The top tested concentration of 0.5 mg/mL represents a concentration higher than necessary for future applications thus it can be concluded based on *in vitro* testing that these systems can be safely applied in a non-toxic manner for purposes such as drug delivery. Furthermore, the observation of *in vitro* cytocompatibility is in agreement with previously published data. [44]

Due to the amphiphilic nature of the polymers generated it was deemed appropriate to investigate their potential to perturb the plasma membrane via LDH release measurements. Amphiphilic surfactant-like compounds have the properties to intercalate with the phospholipid bilayer of the cell plasma membrane, which can result in damage and loss of barrier function. [68,69] Lack of membrane damage as observed with the systems tested here indicates the absence of a toxic membrane-associated effect. However minor, non-destructive effects such as changes in membrane fluidity cannot be ruled out without further investigation. Nevertheless, the data suggest that the polymer NPs systems remain intact in the extracellular media and do not disassemble into polymer units prior to interacting with cell plasma membranes. While out of the scope of current study, future work with these systems shall assess NPs endocytosis, subsequent intracellular degradation in lysosomes and payload release.

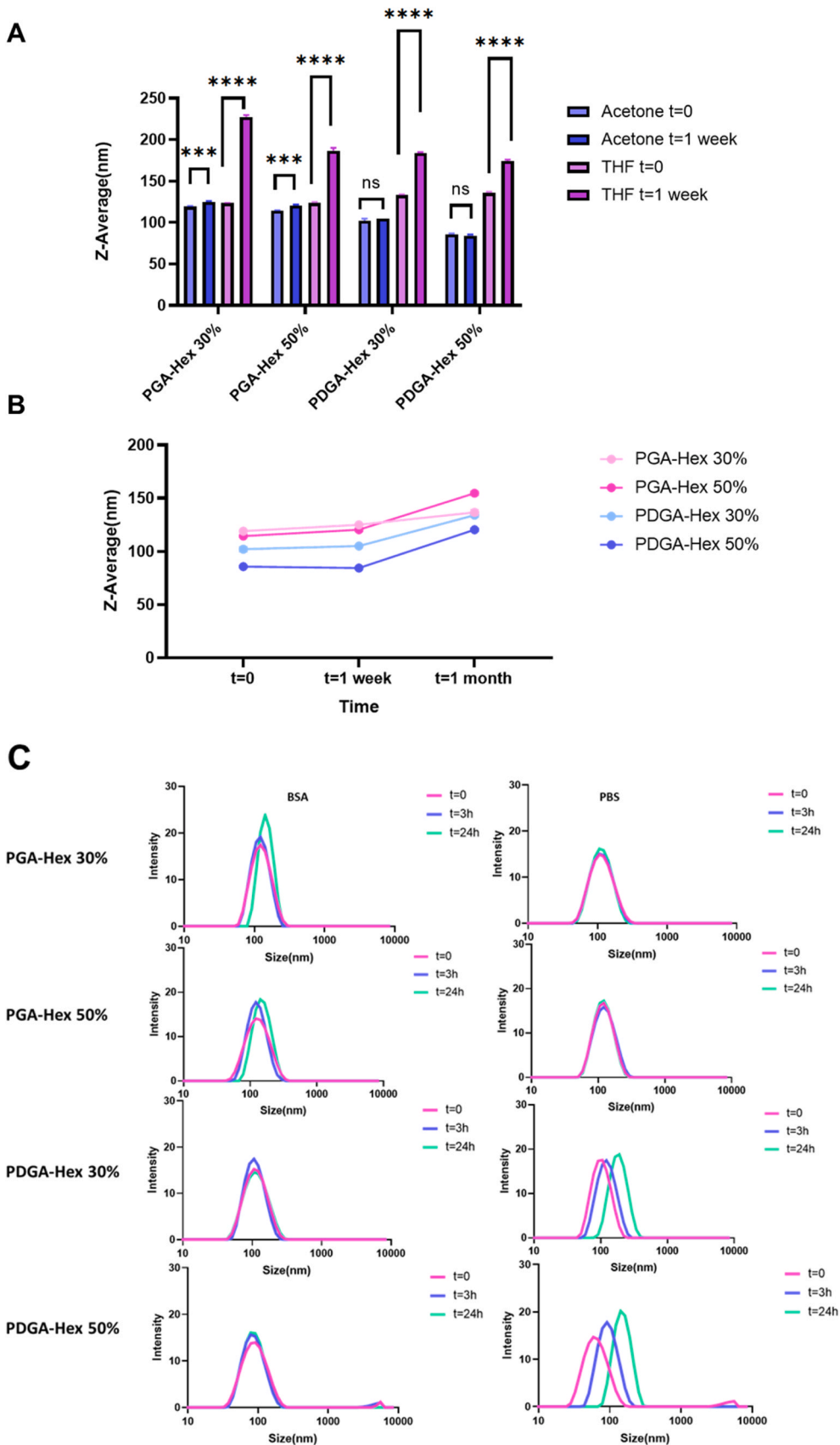


Fig. 2. A. DLS graph presenting the Z-average of the polymers by Intensity. Two solvents were investigated for the NPs production method; Acetone and THF and for two different time points; T=0 and T=1 week. B. DLS sizes trend showing NPs stability over time up to 1 month. C. Demonstration of the DLS results for the stability studies. The stability studies were done using two different media, PBS and BSA.

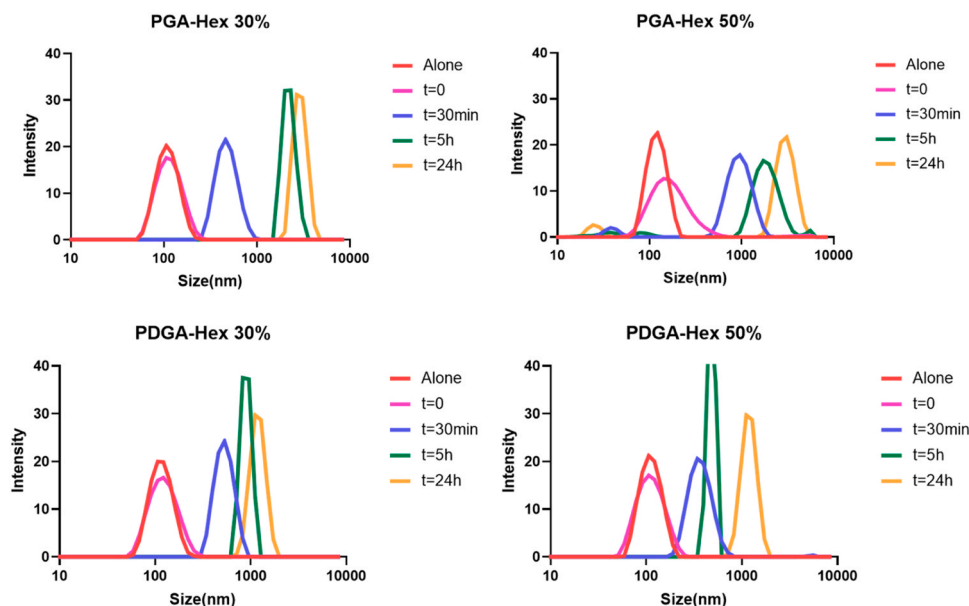


Fig. 3. Demonstration of the DLS results for the degradation studies. All polymers were mixed with a lipase solution in order to investigate their degradation ability through time.

3.9.2. In vivo: organism viability

C. elegans is a simple model organism used to test biocompatibility and toxicity for complex biological systems such as humans. [70] In this context, nematodes can be used as suitable organism to evaluate the efficacy and optimisation of nano-formulation systems [71] and includes drug delivery applications. [72,73]

C. elegans viability was determined by observing the motility of adult worms and their ability to produce offspring. Worms that are motile are considered viable, whereas nematodes treated with 20% v/v ethanol are not motile or produce progeny.

The NPs PGA-Hex (30% & 50%) and PDGA-Hex (30% & 50%) did not significantly affect the viability of *C. elegans* compared to M9 and Ethanol (20% v/v) controls after 24 hours of exposure (Fig. 4 C; $P > 0.05$). This observation was supported by similar worm motility between the M9 control and those treated with polymeric NPs, along with the offspring they produced over the 24-hour study (Fig. 4 D and Supplementary video).

In addition, PDGA-Hex 50% displayed visible aggregation after being suspended in M9 buffer solution for 24 hours (PDGA-Hex 50%, Fig. 4 D). This is most likely linked to its reduced stability, in high salt solution also exhibited in data with PBS (Fig. 4C). Nevertheless, a reduction in viability was not observed detected from this sample. These data mirror earlier studies, which highlight that nematodes appear to consume these aggregates without any adverse impact on their viability or reproductive capabilities. [44]

3.9.3. Model drug encapsulation screening

The ability of the polymeric NPs to encapsulate a hydrophobic model compound was evaluated. Coumarin 6 (Cou6) is a fluorescent, water-insoluble small molecule that has previously been used in encapsulation studies as a model hydrophobic compound with a drug-like structure to mimic the behaviour of lipophilic active ingredients. [44] Cou6 was co-nanoprecipitated with and without (control) polymers. (Fig. 5A). The apparent solubility of the drug-like Cou6 in water was determined in a fast and semi-quantitative fashion by using $\Delta F\%$. The polymers were then ranked according to their $\Delta F\%$ value, which is directly related to the enhancement of the water apparent solubility of Cou6. Previously, the differences in UV-vis Absorbance ($\Delta A\%$) was adopted as direct measurement of the water apparent solubility of Cou6. However, in this case we opted for analysing the dye fluorescence signal due to the

negligible polymer effect and a better final detection of the dye signal.

After Cou6 encapsulation, a drop in zeta potential from around -25 mV to circa -30 mV for all the polymers in was observed in agreement with previous studies on similar polymers. This might also be due to more hydrophobic interaction between cou6 and NP core, resulting in more compacted core of NPs compared to blank NPs and higher negative ZP. More hydrophobic interaction of NP core may expel more hydroxyl groups to present on the NP surface and drop the ZP to more negative value. PGA-Hex 30% and PGA-Hex 50% showed lower $\Delta F\%$ (more than half compared to the PDGA polymers) values compared to their PDGA-Hex modified counterparts (Fig. 5A). The increase in apparent solubility of Cou6 in the PDGA-Hex 30% and 50% formulations, as previously found for PDGA-Hex 50% alone, this is attributed to an enhancement in the amphiphilicity of the polymeric backbones, the greater hydrogen bond interactions from additional hydroxyl functionalities (due to diglycerol), as well as the less hydrophobic and looser core. This latter is the consequence of lower hydrophobic interactions inside the NPs core with consequent availability to host more dye, and therefore higher $\Delta F\%$. Upon analysis of the best performing NPs, it is observed that sizes after Cou6 encapsulation tended to slightly contract (seen by both TEM and DLS, Fig. 5B and C). This is likely due to the stronger interactions between the polymer chain, the hydroxyl group in the side chain with the drug molecule.

Finally, by selecting the nanoprecipitation as a formulation strategy, spherical NPs were produced as confirmed by TEM analysis (Fig. 5B). However, for all the samples analysed, some aggregation occurred, and therefore, heterogeneity in the size distributions was observed. This was more evident for PDGA-Hex30% since this polymer showed only a T_g around -28 °C, while PDGA-Hex 50% showed a T_g below -38 °C but multiple T_m s above room temperature. In this regard, it has been shown that soft materials with low T_g , tend to flow, migrate, and aggregate during drying and during TEM analysis. [74] To better analyse these systems and avoid artifacts, Cryo-TEM analysis will be performed in the future.

4. Conclusion

In this work, we investigated the effects of purification steps and variations in the stoichiometry of monomer feed ratio on the amphiphilicity balance of glycerol/dyglycerol-based polyester backbones,

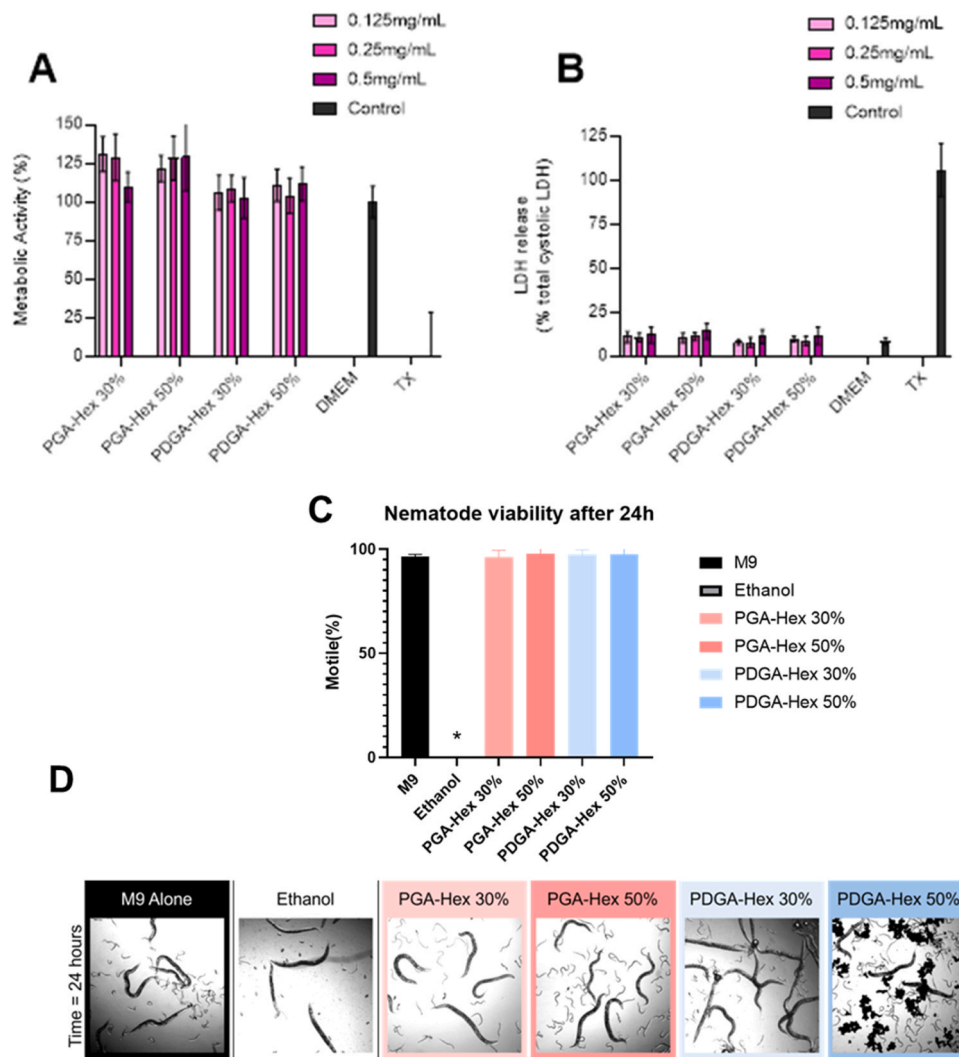


Fig. 4. Cytotoxicity of tested polymeric systems in Caco-2 intestinal cells assessed via **A.** metabolic activity using PrestoBlue assay and **B.** LDH release assay. Cells exposed for 24 hours to varying concentrations of polymeric systems and DMEM culture media as vehicle control and 1% (v/v) Triton X-100 (TX) as cell death inducing control. Data presented as mean \pm S.D. **C.** *C. elegans* viability, as a function of motility, after 24 h challenge with NPs at 0.5 mg/mL. Experiments were conducted in triplicate per formulation with >40 nematodes per experiment analysed. No significant differences in viability were observed ($P > 0.05$), except for those nematodes treated with ethanol ($* = P < 0.001$). **D.** Brightfield microscopy images of nematodes after exposure to polymeric NPs. Nematode progeny was observed in control maintenance M9 alone and PGA-Hex (30% & 50%) and PDGA-Hex (30% & 50%) treated suspensions after 24 h of exposure, indicative of nematode viability. Progeny were not observed for nematodes treated with ethanol 20% v/v. See supporting video S1 for confirmation of nematode motility as an indicator of viability.

prepared using a one-pot, one-step enzymatic polycondensation process. We examined their impact on nanoparticle properties, including nanoparticle formation, stability and drug encapsulation. It was found that by changing the (hydrophilic) polyol: (hydrophobic) diol feed ratio, polymers with different properties could be prepared in mild and sustainable conditions. The variation of the chain amphiphilicity allows the fine tuning of NPs stability in biologically relevant media, as well as drug encapsulation efficiency. Combined with the assessed biodegradability and the absence of cytotoxicity *in vitro* experiments as well as *in vivo* whole organism models, this work shows promising potential for further screening of these polymers and new variations as nano-drug delivery carriers. Although PDGA-Hex 30% proved to be the best candidate, by balancing good stability in relevant media and good dye encapsulation, a clear candidate has not been underpinned due to the limited number of the polymers analysed. However, the promising results, reported in this work, can be pivotal for more works in this area and to broaden interest towards more sustainably sourced and synthesised PEG-free polyesters.

CRediT authorship contribution statement

Benoit Coutraud: Writing – review & editing, Writing – original draft, Visualization, Methodology. **Daniel J. Keddie:** Writing – review & editing, Writing – original draft, Visualization, Validation. **Sadie M.E. Swainson:** Writing – review & editing, Visualization, Validation, Methodology. **Jiraphong Suksiriworapong:** Writing – review & editing, Writing – original draft, Visualization, Methodology. **Steven M. Howdle:** Writing – review & editing, Visualization, Supervision. **Iolanda Francolini:** Writing – review & editing, Writing – original draft, Validation, Supervision, Methodology, Investigation, Conceptualization. **Robert J. Cavanagh:** Writing – review & editing, Writing – original draft, Visualization, Supervision, Resources, Methodology, Investigation, Data curation. **Emily G. Dixon:** Writing – review & editing, Writing – original draft, Visualization, Resources, Methodology, Formal analysis, Data curation. **Philippa L. Jacob:** Writing – review & editing, Writing – original draft, Visualization, Methodology, Data curation, Conceptualization. **Eleni Axioti:** Writing – review & editing,

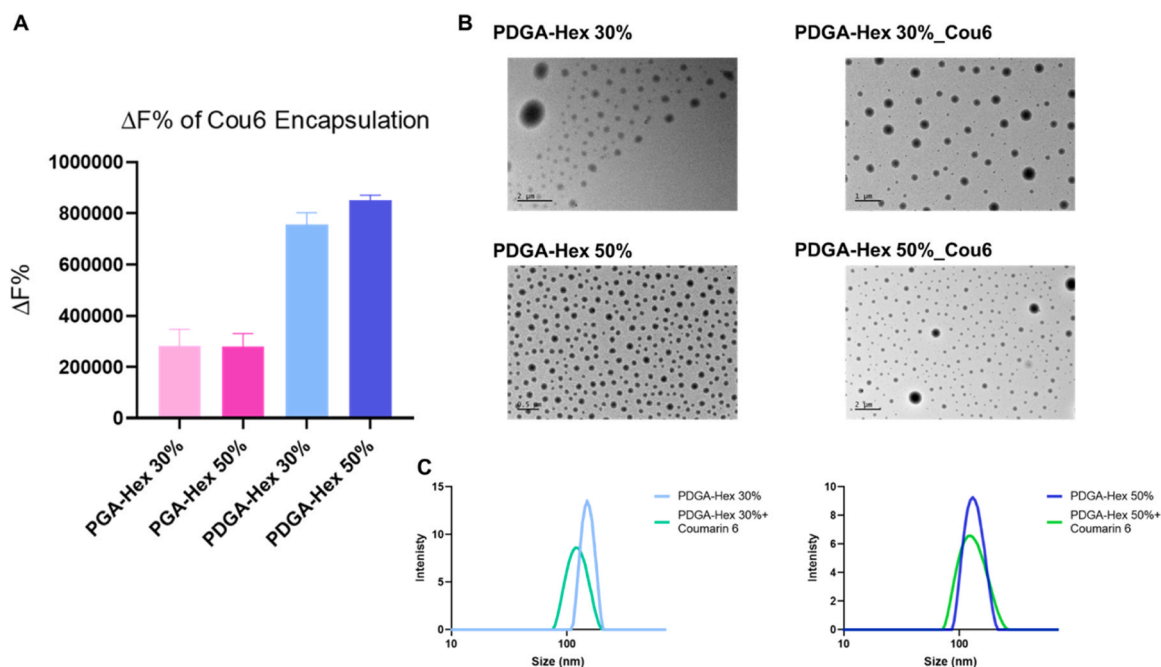


Fig. 5. A. $\Delta F\%$ ranking of Cou6 against PGA-Hex 30%, PGA-Hex 50%, PDGA-Hex 30% and PDGA-Hex 50%. B. TEM images of PDGA-Hex 30% alone and with Cou6, PDGA-Hex 50% alone and with Cou6. C. DLS traces showing the size distribution of PDGA-Hex 30% (left) and PDGA-Hex 50% (right) as free polymers against the corresponding polymers after encapsulation of Cou6.

Writing – original draft, Visualization, Software, Methodology, Formal analysis, Data curation. **Vincenzo Taresco:** Writing – review & editing, Writing – original draft, Validation, Supervision, Resources, Project administration, Investigation, Funding acquisition, Formal analysis, Data curation, Conceptualization. **Euan C. H. Alexander:** Writing – review & editing, Methodology, Investigation, Data curation. **Morgan Reynolds-Green:** Writing – review & editing, Methodology, Formal analysis, Data curation. **Veeran M. Chauhan:** Writing – review & editing, Writing – original draft, Visualization, Validation, Methodology, Investigation, Formal analysis, Data curation. **Benedetta Brugnoli:** Writing – review & editing, Methodology, Investigation, Formal analysis, Data curation.

Declaration of Competing Interest

The authors declare that they have no known competing financial interests or personal relationships that could have appeared to influence the work reported in this paper.

Data availability

Data will be made available on request.

Acknowledgements

PLJ acknowledges EPSRC/SFI CDT in Sustainable Chemistry – Atoms 2 Products (EP/S022236/1) as well as the EPSRC Doctoral Prize Fellowship (EP/W524402/1) for their funding support. VT and VMC would like to thank the University of Nottingham for their Nottingham Research Fellowship. We are indebted to Shazad Aslam and Dr Kevin Butler (University of Nottingham) for their technical expertise in NMR spectroscopy. JS would like to thank National Research Council of Thailand (NRCT) and Mahidol University [Grant number: N41A640155] for funding support. IF and BB would like to thank the Sapienza University of Rome for its funding support (Grant number RG12218166483FFD). We thank the Nanoscale and Microscale Research Centre (nmRC) at the University of Nottingham for providing

access to instrumentation and Ms. Denise McLean for technical assistance.

Appendix A. Supporting information

Supplementary data associated with this article can be found in the online version at [doi:10.1016/j.colsurfb.2024.113828](https://doi.org/10.1016/j.colsurfb.2024.113828).

References

- [1] B. Kaupbayeva, A.J. Russell, *Prog. Polym. Sci.* 101 (2020) 101194.
- [2] M. Dirauf, I. Muljajew, C. Weber, U.S. Schubert, *Prog. Polym. Sci.* 129 (2022) 101547.
- [3] H. Tian, Z. Tang, X. Zhuang, X. Chen, X. Jing, *Prog. Polym. Sci.* 37 (2012) 237–280.
- [4] R.P. Brannigan, A.P. Dove, *Biomater. Sci.* 5 (2017) 9–21.
- [5] K.E. Washington, R.N. Kularatne, V. Karmegam, M.C. Biewer, M.C. Stefan, *WIREs Nanomed. Nanobiotechnol.* 9 (2017) e1446.
- [6] M. Sokolsky-Papkov, K. Agashi, A. Olaye, K. Shakesheff, A.J. Domb, *Adv. Drug Deliv. Rev.* 59 (2007) 187–206.
- [7] I. Manavitehrani, A. Fathi, H. Badr, S. Daly, A. Negahi Shirazi, F. Dehghani, *Polymers* 8 (2016) 20.
- [8] S.M.E. Swainson, V. Taresco, A.K. Pearce, L.H. Clapp, B. Ager, M. McAllister, C. Bosquillon, M.C. Garnett, *Eur. J. Pharm. Biopharm.* 142 (2019) 377–386.
- [9] A. Rosato, A. Romano, G. Totaro, A. Celli, F. Fava, G. Zanaroli, L. Sisti, *Polymers* 14 (2022) 1850.
- [10] A.K. Pearce, R.K. O'Reilly, *Biomacromolecules* 22 (2021) 4459–4469.
- [11] M. Vert, *Biomacromolecules* 6 (2005) 538–546.
- [12] N. Singh, A. Joshi, A.P. Toor, G. Verma, in: *Nanostructures for Drug Delivery*, Elsevier, 2017, pp. 865–886.
- [13] M.A. Hillmyer, W.B. Tolman, *Acc. Chem. Res.* 47 (2014) 2390–2396.
- [14] H. Seyednejad, A.H. Ghassemi, C.F. van Nostrum, T. Vermonden, W.E. Hennink, *J. Control. Release* 152 (2011) 168–176.
- [15] X. Wang, Z. Zhang, N. Hadjichristidis, *Prog. Polym. Sci.* 136 (2023) 101634.
- [16] H. Kweon, M.K. Yoo, I.K. Park, T.H. Kim, H.C. Lee, H.-S. Lee, J.-S. Oh, T. Akaike, C.-S. Cho, *Biomaterials* 24 (2003) 801–808.
- [17] T.T. Hoang Thi, E.H. Pilkington, D.H. Nguyen, J.S. Lee, K.D. Park, N.P. Truong, *Polym. (Basel)* 12 (2020).
- [18] M. Ibrahim, E. Ramadan, N.E. Elsadek, S.E. Emam, T. Shimizu, H. Ando, Y. Ishima, O.H. Elgarhy, H.A. Sarhan, A.K. Hussein, T. Ishida, *J. Control. Release* 351 (2022) 215–230.
- [19] N.E. Elsadek, A.S. Abu Lila, T. Ishida, in: *Polymer-Protein Conjugates*, Elsevier, 2020, pp. 103–123.
- [20] X. Yao, C. Qi, C. Sun, F. Huo, X. Jiang, *Nano Today* 48 (2023) 101738.
- [21] A.S. Dutta, in: *Recycling of Polyurethane Foams*, William Andrew Publishing, 2018, pp. 17–27.
- [22] K. Lang, R.J. Sánchez-Leija, R.A. Gross, R.J. Linhardt, *Polym. (Basel)* 12 (2020).

- [23] R.A. Gross, M. Ganesh, W. Lu, Trends Biotechnol. 28 (2010) 435–443.
- [24] A. Mahapatro, B. Kalra, A. Kumar, R.A. Gross, Biomacromolecules 4 (2003) 544–551.
- [25] C.R. Chilakamarry, A.M.M. Sakinah, A.W. Zularisam, A. Pandey 1 (2021) 378–396.
- [26] V. Hevilla, A. Sonseca, C. Echeverría, A. Muñoz-Bonilla, M. Fernández-García, Macromol. Biosci. 21 (2021) 2100156.
- [27] F. Zeng, X. Yang, D. Li, L. Dai, X. Zhang, Y. Lv, Z. Wei, J. Appl. Polym. Sci. 137 (2019) 48574.
- [28] B. Parshad, M. Kumari, V. Khatri, R. Rajeshwari, Y. Pan, A. Sharma, I. Ahmed, Eur. Polym. J. 158 (2021) 110690.
- [29] V. Taresco, J. Suksiriworapong, R. Creasey, J.C. Burley, G. Mantovani, C. Alexander, K. Treacher, J. Booth, M.C. Garnett, J. Polym. Sci. Part A: Polym. Chem. 54 (2016) 3267–3278.
- [30] V. Taresco, J. Suksiriworapong, I.D. Styliari, R.H. Argent, Sadie M.E. Swainson, J. Booth, E. Turpin, C.A. Loughton, J.C. Burley, C. Alexander, M.C. Garnett, RSC Adv. 6 (2016) 109401–109405.
- [31] G. Du, D. Belić, A. Del Giudice, V. Alfredsson, A.M. Carnerup, K. Zhu, B. Nyström, Y. Wang, L. Galantini, K. Schillén, Angew. Chem. Int. Ed. Engl. 61 (2022) e202113279.
- [32] J. Cautela, B. Stenqvist, K. Schillén, D. Belić, L.K. Månsson, F. Hagemans, M. Seuss, A. Fery, J.J. Crassous, L. Galantini, ACS Nano 14 (2020) 15748–15756.
- [33] G.B. Perin, M.I. Felisberti, Macromolecules 56 (2023) 6968–6977.
- [34] T. Naolou, V.M. Weiss, D. Conrad, K. Busse, K. Mäder, J. Kressler, in *Tailored Polymer Architectures for Pharmaceutical and Biomedical Applications*, vol. 1135, American Chemical Society, 2013, pp. 39–52.
- [35] S.M.E. Swainson, I.D. Styliari, V. Taresco, M.C. Garnett, Polymers 11 (2019) 1561.
- [36] V. Taresco, R.G. Creasey, J. Kennon, G. Mantovani, C. Alexander, J.C. Burley, M. C. Garnett, Polymer 89 (2016) 41–49.
- [37] T. Attarbach, M.D. Kingsley, V. Spallina, Fuel 340 (2023) 127485.
- [38] V. Hevilla, A. Sonseca, C. Echeverría, A. Muñoz-Bonilla, M. Fernández-García, Eur. Polym. J. 186 (2023) 111875.
- [39] J. Suksiriworapong, V. Taresco, D.P. Ivanov, I.D. Styliari, K. Sakchaisri, V. B. Junyaprasert, M.C. Garnett, Colloids Surf. B Biointerfaces 167 (2018) 115–125.
- [40] K. Damrongrak, K. Kloysawat, S. Bunsupa, K. Sakchaisri, A. Wongrakpanich, V. Taresco, V. Cuzzucoli Crucitti, M.C. Garnett, J. Suksiriworapong, Int. J. Pharm. 618 (2022) 121636.
- [41] J. Suksiriworapong, C. Achayawat, P. Juangrattanajakorn, V. Taresco, V. C. Crucitti, K. Sakchaisri, S. Bunsupa, Pharmaceutics 15 (2023) 2100.
- [42] J. Suksiriworapong, N. Pongprasert, S. Bunsupa, V. Taresco, V.C. Crucitti, T. Januraj, P. Phruttiwanichakun, K. Sakchaisri, A. Wongrakpanich, Pharmaceutics 15 (2023) 1771.
- [43] P. Jacob, L. Ruiz, A. Pearce, Y. He, J.C. Lentz, J. Moore, F. Machado, G. Rivers, E. Apebende, M. Romero Fernandez, I. Francolini, R. Wildman, S. Howdle, V. Taresco, Polymer 228 (2021) 123912.
- [44] P.L. Jacob, B. Brugnoti, A. Del Giudice, H. Phan, V.M. Chauhan, L. Beckett, R. B. Gillis, C. Moloney, R.J. Cavanagh, E. Krumins, M. Reynolds-Green, J.C. Lentz, C. Conte, V. Cuzzucoli Crucitti, B. Couturaud, L. Galantini, I. Francolini, S. M. Howdle, V. Taresco, J. Colloid Interface Sci. 641 (2023) 1043–1057.
- [45] V. Taresco, I. Tulini, I. Francolini, A. Piozzi, Int. J. Mol. Sci. 23 (2022) 14339.
- [46] V.M. Chauhan, G. Orsi, A. Brown, D.I. Pritchard, J.W. Aylott, ACS Nano 7 (2013) 5577–5587.
- [47] K. Ślusarczyk, M. Flejszar, P. Chmielarz, Green. Chem. 25 (2023) 522–542.
- [48] Y. Mei, K. Chen, J. Gu, J. Ling, X. Ni, Green. Chem. 25 (2023) 934–939.
- [49] G. Englezou, K. Kortsen, A.A.C. Pacheco, R. Cavanagh, J.C. Lentz, E. Krumins, C. Sanders-Velez, S.M. Howdle, A.J. Nedoma, V. Taresco, J. Polym. Sci. 58 (2020) 1571–1581.
- [50] P. Kallinteri, S. Higgins, G.A. Hutcheon, C.B. St. Pourçain, M.C. Garnett, Biomacromolecules 6 (2005) 1885–1894.
- [51] Y. Wang, G.A. Ameer, B.J. Sheppard, R. Langer, Nat. Biotechnol. 20 (2002) 602–606.
- [52] Y. Ma, W. Zhang, Z. Wang, Z. Wang, Q. Xie, H. Niu, H. Guo, Y. Yuan, C. Liu, Acta Biomater. 44 (2016) 110–124.
- [53] G.B. Perin, M.I. Felisberti, Macromolecules 53 (2020) 7925–7935.
- [54] G.B. Perin, M.I. Felisberti, Biomacromolecules 23 (2022) 2968–2975.
- [55] D. Pfefferkorn, M. Pulst, T. Naolou, K. Busse, J. Balko, J. Kressler, J. Polym. Sci. Part B: Polym. Phys. 51 (2013) 1581–1591.
- [56] T. Wersig, M.C. Hacker, J. Kressler, K. Mäder, Int. J. Pharm. 531 (2017) 225–234.
- [57] K.-Y. Law, J. Phys. Chem. Lett. 5 (2014) 686–688.
- [58] A. Zielińska, F. Carreiró, A.M. Oliveira, A. Neves, B. Pires, D.N. Venkatesh, A. Durazzo, M. Lucarini, P. Eder, A.M. Silva, A. Santini, E.B. Souto, Molecules 25 (2020).
- [59] H. Phan, R.I. Minut, P. McCrorie, C. Vasey, R.R. Larder, E. Krumins, M. Marlow, R. Rahman, C. Alexander, V. Taresco, A.K. Pearce, J. Polym. Sci. Part A: Polym. Chem. 57 (2019) 1801–1810.
- [60] M. Beck-Broichsitter, Colloids Surf. A: Physicochem. Eng. Asp. 625 (2021) 126928.
- [61] A.M. de Oliveira, E. Jäger, A. Jäger, P. Stepánek, F.C. Giacomelli, Colloids Surf. A: Physicochem. Eng. Asp. 436 (2013) 1092–1102.
- [62] H. Polat, M.C. Eren, M. Polat, Colloids Surf. A: Physicochem. Eng. Asp. 631 (2021) 127712.
- [63] C.L. Oliveira, F. Veiga, C. Varela, F. Roleira, E. Tavares, I. Silveira, A.J. Ribeiro, Colloids Surf. B: Biointerfaces 150 (2017) 326–333.
- [64] R. Martínez, M.F. Navarro Poupard, A. Álvarez, E. Soprano, M. Migliavacca, C. Carrillo-Carrión, E. Polo, B. Pelaz, P. d Pino, in: *Nanoparticles for Biomedical Applications*, Elsevier, 2020, pp. 5–18.
- [65] M.G. Soliman, B. Pelaz, W.J. Parak, P. del Pino, Chem. Mater. 27 (2015) 990–997.
- [66] N. Bizmark, M.A. Ioannidis, Langmuir 31 (2015) 9282–9289.
- [67] C. Colombo, L. Dragoni, S. Gatti, R.M. Pesce, T.R. Rooney, E. Mavroudakis, R. Ferrari, D. Moscatelli, Ind. Eng. Chem. Res. 53 (2014) 9128–9135.
- [68] R.J. Cavanagh, P.A. Smith, S. Stolnik, Mol. Pharm. 16 (2019) 618–631.
- [69] D. Vilasaliu, S. Shubber, R. Fowler, M. Garnett, C. Alexander, S. Stolnik, J. Pharm. Sci. 102 (2013) 114–125.
- [70] P.R. Hunt, J. Appl. Toxicol. 37 (2017) 50–59.
- [71] F. Côa, L. d S. Bortolozzo, D.S. Ávila, A.G. Souza Filho, D.S.T. Martinez, Front. Carbon 2 (2023).
- [72] M.A. Al-Natour, M.D. Yousif, R. Cavanagh, A. Abouselo, E.A. Apebende, A. Ghaemmaghami, D.-H. Kim, J.W. Aylott, V. Taresco, V.M. Chauhan, C. Alexander, ACS Macro Lett. 9 (2020) 431–437.
- [73] B. Brugnoti, A. Mariano, B. Simonis, C. Bombelli, S. Sennato, A. Piozzi, V. Taresco, V.M. Chauhan, S.M. Howdle, A. Scotto d’Abusco, I. Francolini, Carbohydr. Polym. Technol. Appl. 6 (2023) 100373.
- [74] J.-L.P. Vanessa Durrieu, Raphaël Passas, Alessandro Gandini, Cryoelectron Microsc. 18 (2004) 19–21.